

# Interacting Boson Models of Nuclear and Nucleon Structure

## Modelos de Bosones Interactuantes de la Estructura Nuclear y Nucleónica \*

R. Bijker

Instituto de Ciencias Nucleares,  
Universidad Nacional Autónoma de México,  
A.P. 70-543, 04510 México, D.F., México

A. Leviatan

Racah Institute of Physics, The Hebrew University,  
Jerusalem 91904, Israel

**ABSTRACT:** Interacting boson models provide an elegant and powerful method to describe collective excitations of complex systems by introducing a set of effective degrees of freedom. We review the interacting boson model of nuclear structure and discuss a recent extension to the nucleon and its excited states.

**RESUMEN:** Los modelos de bosones interactuantes proveen un método elegante y eficaz para describir excitaciones colectivas de sistemas complejos mediante la introducción de grados de libertad efectivos. Primero revisamos el modelo de bosones interactuantes de la estructura nuclear y luego presentamos una extensión a la estructura del nucleón y sus estados excitados.

PACS: 03.65.Fd, 21.10.Re, 21.60.Ev, 14.20.Gk

---

\*Plática plenaria invitada en el ‘XL Congreso Nacional de Física’, Monterrey, Nuevo León, 27 - 31 de octubre de 1997

# 1 Introduction

Atomic nuclei are complex systems consisting of large numbers of strongly interacting protons and neutrons and involving many degrees of freedom. In addition, the nucleons themselves are composite particles, each including three valence quarks. In principle, the structure and interactions of nucleons are described by quantum chromodynamics (QCD) of quarks and gluons which has emerged as the fundamental theory of strong interactions. However, the energy domain of nuclear physics, several MeV's ( $= 10^6$  eV's) for nuclear structure and several GeV's ( $= 10^9$  eV's) for excitations of the nucleon, belongs to the nonperturbative regime of QCD for which, except for lattice calculations of ground state properties, no reasonable solution exists.

Nevertheless, the low-lying spectrum of many nuclei exhibits a surprisingly simple structure. In the absence of an exactly solvable theory and reliable approximation methods, one has to rely on models of nuclear structure and symmetries to ‘understand’ these regular features. In models one attempts to isolate the most important degrees of freedom and deal with them explicitly. Examples of nuclear models are the shell model in which the complicated motion of nucleons inside a nucleus is replaced by the motion of independent nucleons in a static spherical potential well [1], the collective or geometric model in which collective nuclei are described in terms of geometric variables that characterize the shape and deformation of the nuclear surface [2], and the interacting boson model in which collective quadrupole states in nuclei are described in terms of a system of interacting monopole and quadrupole bosons [3].

Whereas in low energy nuclear physics it is a good approximation to neglect the internal structure of the nucleon, this is no longer the case for excitations of the nucleon itself (baryon resonances). Nowadays the nucleon is viewed as a confined system of quarks interacting via gluon exchange. Effective models of the nucleon are all based on three constituent parts that carry the internal degrees of freedom of spin, flavor and color [4], but differ in their treatment of radial (or orbital) excitations. At the same time, the baryon mass spectrum shows some remarkable regularities, such as linear Regge trajectories and parity doublets, which indicates that a collective type of dynamics may play an important role in the structure of baryons.

In this contribution we show that interacting boson models provide an elegant and, at the same time, powerful method to describe collective excitations of complex systems by introducing a set of effective degrees of freedom. We first review the main features of the interacting boson model of nuclear structure, and next discuss a recent extension to the nucleon and its excited states.

## 2 Nuclear structure

The nuclear shell model has been very successful in describing and correlating a vast amount of experimental data. In this model it is assumed that each nucleon (proton or neutron) moves independently in a static spherical potential that represents the average interaction with other nucleons in the nucleus. The ordering of single nucleon levels (or orbits) is shown schematically in Figure 1. The single nucleon orbits which, due to the Pauli exclusion principle, can only be occupied by a restricted number of identical nucleons are clustered into major shells. The number of protons or neutrons in a completely filled major shell is called a magic number. Doubly-magic nuclei with completely filled proton and neutron major shells are particularly stable. The shell model correctly reproduces all observed magic numbers.

The lowest excited states of a nucleus with one nucleon outside a closed shell are obtained by the extra (or valence) nucleon occupying the various orbits in the next major shell. As an example we show in Figure 2 the observed energy levels of the nucleus  $^{209}_{82}\text{Pb}_{127}$  together with their shell model interpretation as a valence neutron occupying the single-particle orbits  $2g_{9/2}$ ,  $1i_{11/2}$ ,  $1j_{15/2}$ ,  $3d_{5/2}$ ,  $4s_{1/2}$   $2g_{7/2}$  and  $3d_{3/2}$  of the 126-184 major shell.

The size of the model space increases rapidly if there are both protons and neutrons outside closed shells. As an example, we consider the nucleus  $^{154}_{62}\text{Sm}_{92}$ , which has 12 valence protons occupying the single-particle orbits  $1g_{7/2}$ ,  $2d_{5/2}$ ,  $2d_{3/2}$ ,  $3s_{1/2}$  and  $1h_{11/2}$  of the 50-82 major shell and 10 valence neutrons occupying the orbits  $1h_{9/2}$ ,  $2f_{7/2}$ ,  $2f_{5/2}$ ,  $3p_{3/2}$ ,  $3p_{1/2}$  and  $1i_{13/2}$  of the 82-126 major shell. Even with the assumption that the lowest excited states of this nucleus can be described by taking into account only the valence nucleons, the shell model space is enormous [1], as can be seen from the first column of Table 1. Despite the enormous size of the model space, the low-lying spectrum of  $^{154}\text{Sm}$  shows a remarkably regular pattern. This suggests the existence of ‘effective’ degrees of freedom, which would truncate the large shell model space to a manageable size, but without losing the simple features of the energy spectrum.

Such an alternative is provided by the interacting boson model of nuclei. Its microscopic basis is the observation that the interaction between identical nucleons favors the formation of monopole and quadrupole pairs of nucleons. The interacting boson model can be viewed as a truncated shell model, in which the large shell model space spanned by the valence nucleons is truncated to the subspace spanned by monopole and quadrupole pairs of identical nucleons, which subsequently are treated as bosons.

### 2.1 The interacting boson model

In the original formulation of the interacting boson model (IBM-1) no distinction is made between proton and neutron degrees of freedom. Low-lying collective states in even-even nuclei are described in terms of a system of  $N$  interacting bosons with angular momentum and parity  $L^P = 0^+$  (monopole) and  $L^P = 2^+$

(quadrupole). Since the five components of the quadrupole boson and the monopole boson span a six-dimensional space with group structure  $U(6)$ , all states belong to the symmetric irreducible representation  $[N]$  of  $U(6)$ , where  $N$  is the total number of bosons. In the IBM the Hamiltonian is expressed in second quantization. Hereto we introduce creation operators,  $s^\dagger$  and  $d_m^\dagger$ , and annihilation operators,  $s$  and  $d_m$ , for the bosons, which altogether can be denoted by  $b_{lm}^\dagger$  and  $b_{lm}$  with  $l = 0, 2$  and  $m = -l, -l+1, \dots, l$

$$b_{00}^\dagger \equiv s^\dagger, \quad b_{2m}^\dagger \equiv d_m^\dagger. \quad (1)$$

The operators  $b_{lm}^\dagger$  and  $b_{lm}$  satisfy standard boson commutation relations

$$[b_{l_1 m_1}, b_{l_2 m_2}^\dagger] = \delta_{l_1 l_2} \delta_{m_1 m_2}, \quad [b_{l_1 m_1}^\dagger, b_{l_2 m_2}^\dagger] = [b_{l_1 m_1}, b_{l_2 m_2}] = 0. \quad (2)$$

In second quantized form, the most general one- and two-body rotational invariant Hamiltonian that conserves the number of bosons is given by

$$H = H_0 + \sum_l \epsilon_l \sum_m b_{lm}^\dagger b_{lm} + \sum_L \sum_{l_1 l_2 l_3 l_4} v_{l_1 l_2 l_3 l_4}^{(L)} (b_{l_1}^\dagger \times b_{l_2}^\dagger)^{(L)} \cdot (\tilde{b}_{l_3} \times \tilde{b}_{l_4})^{(L)}, \quad (3)$$

with  $\tilde{b}_{lm} = (-1)^{l-m} b_{l,-m}$ . The dots indicate scalar products and the crosses tensor products. Since the monopole and quadrupole bosons are identified with correlated pairs of valence nucleons, the number of bosons  $N$  is determined by the total number of active proton and neutron pairs, counted from the nearest closed shell.

As an example, the nucleus  $^{154}_{62}\text{Sm}_{92}$ , where the 12 valence protons occupy the 50-82 proton shell and the 10 valence neutrons occupy the 82-126 neutron shell, is treated in the IBM as a system of  $N = 6 + 5 = 11$  interacting bosons. The number of states with angular momentum and parity  $L^P = 0^+$ ,  $2^+$  and  $4^+$  is reduced from the shell model values by a factor  $10^{12} - 10^{13}$  (see Table 1). This reduction makes it possible to study low-lying collective excitations in nuclei by diagonalizing Hamiltonian matrices of relatively small dimensions. In the last column of Table 1 we show the dimensions of the model space in the neutron-proton interacting boson model (IBM-2) in which the neutron-proton degrees of freedom are taken into account explicitly.

## 2.2 Dynamical symmetries

In general, the Hamiltonian matrix can be diagonalized numerically to obtain the energy eigenvalues, but there exist also limiting situations in which the energy spectra can be obtained in closed analytic form, that is to say, in terms of an energy formula. These special cases correspond to dynamical symmetries, and arise whenever the Hamiltonian can be written in terms of Casimir invariants of a chain of subgroups of  $U(6)$  only [3]. Since nuclear states have good angular momentum, the rotation group  $SO(3)$  in three dimensions should be included in all subgroup chains. Under this restriction there are three possible

chains [3]

$$U(6) \supset \begin{cases} U(5) \supset SO(5) \supset SO(3) , \\ SU(3) \supset SO(3) , \\ SO(6) \supset SO(5) \supset SO(3) . \end{cases} \quad (4)$$

The corresponding dynamical symmetries are usually referred to as the  $U(5)$ , the  $SU(3)$  and the  $SO(6)$  limits, respectively.

(i) In the  $U(5)$  limit, the energy eigenvalues are given by

$$E(n, v, L) = E_0 + \epsilon n + \alpha n(n+4) + \beta v(v+3) + \gamma L(L+1) , \quad (5)$$

where  $n$ ,  $v$  and  $L$  are quantum numbers that label the basis states. Here  $n$  represents the number of quadrupole bosons,  $v$  is the boson seniority, *i.e.* the number of quadrupole bosons not coupled pairwise to angular momentum zero, and  $L$  denotes the angular momentum. The energy spectrum is characterized by a series of multiplets labeled by  $n$  at almost constant energy spacing ( $\alpha, \beta, \gamma \ll \epsilon$ ), which is typical for a vibrational nucleus. The ground state has  $n = v = L = 0$  and energy  $E_0$ . In Fig. 3 we show the structure of a spectrum in the  $U(5)$  limit.

(ii) The energy eigenvalues in the  $SU(3)$  limit are given by

$$E(\lambda, \mu, L) = E_0 - \kappa [\lambda(\lambda+3) + \mu(\mu+3) + \lambda\mu - 2N(2N+3)] + \kappa' L(L+1) . \quad (6)$$

Here  $\lambda$ ,  $\mu$  and  $L$  label the basis states. The spectrum is characterized by a series of bands labeled by  $(\lambda, \mu)$ , in which the energy spacing is proportional to  $L(L+1)$ , as in a rigid rotor model. The ground state band has  $(\lambda, \mu) = (2N, 0)$  for a prolate rotor or  $(\lambda, \mu) = (0, 2N)$  for an oblate rotor. In both cases the ground state energy is  $E_0$ . In Fig. 4 we show a typical spectrum in the  $SU(3)$  limit.

(iii) Finally, the energy formula in the  $SO(6)$  limit is given by

$$E(\sigma, \tau, L) = E_0 + A(N-\sigma)(N+\sigma+4) + B\tau(\tau+3) + C L(L+1) , \quad (7)$$

where  $\sigma$ ,  $\tau$  and  $L$  characterize the basis states. Here  $\sigma$  and  $\tau$  denote boson seniority labels:  $\tau$  has the same meaning as  $v$  in the  $U(5)$  limit, *i.e.* the number of quadrupole bosons not coupled pairwise to angular momentum zero, whereas  $\sigma$  is a generalized seniority that involves both monopole and quadrupole bosons. The energy spectrum consists of a series of vibrational multiplets labeled by  $\sigma$ , in which the energy spacing is proportional to the last two terms in Eq. (7). The ground state has  $\sigma = N$ ,  $\tau = L = 0$  and energy  $E_0$ . In Fig. 5 we show a typical spectrum in the  $SO(6)$  limit.

The three dynamical symmetries provide a set of closed analytic expressions for energies, electromagnetic transition rates and selection rules that can be tested easily by experiment, and as such they play an

important role in the qualitative interpretation of the data. However, only a few nuclei can be described by these limiting situations. We mention the low-lying states of  $^{110}_{48}\text{Cd}_{62}$ ,  $^{156}_{64}\text{Gd}_{92}$  and  $^{196}_{78}\text{Pt}_{118}$  as good examples of nuclei with  $U(5)$ ,  $SU(3)$  and  $SO(6)$  symmetry, respectively [3]. Most nuclei display properties intermediate between the dynamical symmetries. In order to describe transitional regions between any of the three dynamical symmetries, the more general form of the IBM Hamiltonian of Eq. (3) has to be used. Its eigenvalues and eigenvectors can be obtained by numerical diagonalization. As examples of transitional regions we mention the mass region between the Pt isotopes and the well-deformed region of the rare earth nuclei, which has been interpreted in terms of a  $SO(6) \leftrightarrow SU(3)$  transition, the Sm isotopes which show a sharp transition between vibrational and rotational spectra ( $U(5) \leftrightarrow SU(3)$ ) and the Ru isotopes which show a transition between vibrational and  $\gamma$  unstable nuclei ( $U(5) \leftrightarrow SO(6)$ ).

### 2.3 Classical limit

In a geometric model of collective quadrupole excitations of the nucleus, the nuclear surface is described by its radius

$$R = R_0 \left[ 1 + \sum_{\mu} \alpha_{\mu} Y_{2\mu}(\theta, \phi) \right], \quad (8)$$

which is parametrized by five shape variables  $\alpha_{\mu}$  ( $\mu = -2, \dots, 2$ ). Instead of  $\alpha_{\mu}$  it is more convenient to make a transformation to the body-fixed system and to introduce the Hill-Wheeler coordinates  $\beta, \gamma$  which determine the shape, together with the three Euler angles which determine the orientation in space [2].

The connection between the IBM and the geometric model can be obtained by studying the classical limit of the IBM by means of mean-field techniques [5]. For a system of bosons the variational wave function has the form of a coherent state, which is a condensate of  $N$  deformed bosons. For static rotationally invariant problems, the coherent state is characterized by two geometric or classical variables, which one can associate with  $\beta$  and  $\gamma$ . The coherent state is then given by

$$|N; \beta, \gamma\rangle = \frac{1}{\sqrt{N!}} [b_c^{\dagger}(\beta, \gamma)]^N |0\rangle, \quad (9)$$

with

$$b_c^{\dagger}(\beta, \gamma) = \frac{1}{\sqrt{1 + \beta^2}} \left[ s^{\dagger} + \beta \cos \gamma d_0^{\dagger} + \frac{1}{\sqrt{2}} \beta \sin \gamma (d_2^{\dagger} + d_{-2}^{\dagger}) \right]. \quad (10)$$

For a given IBM Hamiltonian we define an energy surface by its expectation value in the coherent state

$$E(\beta, \gamma) \equiv \langle N; \beta, \gamma | :H: |N; \beta, \gamma\rangle. \quad (11)$$

Taking the normal ordered product of the Hamiltonian  $:H:$  amounts to keeping, for each interaction term, only the leading order contribution in the total number of bosons  $N$ . For the one- and two-body

Hamiltonian of Eq. (3) the energy surface is given by

$$E(\beta, \gamma) = a_0 + \frac{N(N-1)}{(1+\beta^2)^2} [a_2\beta^2 + a_3\beta^3 \cos 3\gamma + a_4\beta^4] , \quad (12)$$

where the coefficients  $a_i$  depend on the number of bosons  $N$  and the parameters in the Hamiltonian.

The classical limits of the three dynamical symmetries have a simple geometric interpretation. For the  $U(5)$  limit the energy surface is given by

$$E(\beta, \gamma) = E_0 + \epsilon \frac{N\beta^2}{1+\beta^2} + \alpha \frac{N(N-1)\beta^4}{(1+\beta^2)^2} , \quad (13)$$

whereas for the  $SU(3)$  limit we find

$$E(\beta, \gamma) = E_0 + \kappa \frac{N(N-1)}{(1+\beta^2)^2} [3\beta^4 \mp 4\sqrt{2}\beta^3 \cos 3\gamma + 4] , \quad (14)$$

and for the  $SO(6)$  limit

$$E(\beta, \gamma) = E_0 + A \frac{N(N-1)}{(1+\beta^2)^2} (1-\beta^2)^2 . \quad (15)$$

The energy surfaces for the  $U(5)$  and  $SO(6)$  limits do not depend on the asymmetry parameter  $\gamma$ . For physical values of the parameters ( $\epsilon > 0$  and  $A > 0$ ) they have a minimum at  $\beta = 0$  (spherical shape) and  $\beta^2 = 1$  (deformed shape with  $\gamma$  instability), respectively. For the  $SU(3)$  limit the energy surface depends on both  $\beta$  and  $\gamma$ , and has for  $\kappa > 0$  a minimum at  $\beta = \sqrt{2}$  and  $\gamma = 0$  (axially deformed prolate shape) or at  $\beta = \sqrt{2}$  and  $\gamma = \pi/3$  (axially deformed oblate shape), depending on the sign of the  $\beta^3 \cos 3\gamma$  term. This analysis shows that the  $U(5)$  limit corresponds to an anharmonic vibrator, the  $SU(3)$  limit to an axial rotor with prolate or oblate deformation, and the  $SO(6)$  limit to a  $\gamma$  unstable rotor (or deformed oscillator).

These results are summarized in the phase triangle of Fig. 6, in which the equilibrium shapes corresponding to each one of the dynamical symmetries are located at the corners, and the transitional regions between any two of them along the three sides. Most nuclei correspond to either the edges or the interior of the triangle, since they are intermediate between two or three limiting situations.

### 3 Nucleon structure

The nucleon itself is not an elementary particle, but a composite object. Effective models of the nucleon and its excited states (or baryon resonances) based on three constituents share a common spin-flavor-color structure but differ in their assumptions on the spatial dynamics. Stimulated by the success of algebraic methods in nuclear [3] and molecular [6] spectroscopy, we discuss here an interacting boson model for the spatial degrees of freedom [7]. This model unifies various exactly solvable models of baryon structure, and hence provides a general framework to study the properties of baryon resonances in a transparent and systematic way.

### 3.1 Algebraic model of the nucleon

Baryons are considered to be built of three constituent parts. The internal degrees of freedom of these three parts are taken to be: flavor-triplet  $u, d, s$  (we do not consider here heavy quark flavors), spin-doublet  $S = 1/2$ , and color-triplet. The internal algebraic structure of the constituent parts is the usual

$$\mathcal{G}_i = SU_{sf}(6) \otimes SU_c(3) \supset SU_f(3) \otimes SU_s(2) \otimes SU_c(3) . \quad (16)$$

In Table 2 we present the classification of the baryon flavor octet and decuplet in terms of the isospin  $I$  and the hypercharge  $Y$  according to the decomposition  $SU_f(3) \supset SU_I(2) \otimes U_Y(1)$ . The hypercharge is related to the electric charge  $Q$  and the third component of the isospin  $I_3$  through the Gell-Mann and Nishijima relation

$$Q = I_3 + \frac{Y}{2} . \quad (17)$$

The strangeness  $S$  is the difference between the hypercharge and the baryon number  $B$

$$S = Y - B . \quad (18)$$

The nucleon and  $\Delta$  are nonstrange  $S = 0$ , whereas the  $\Sigma, \Lambda, \Xi$  and  $\Omega$  hyperons carry strangeness  $S = -1, -1, -2$  and  $-3$ , respectively.

The relative motion of the three constituent parts is described in terms of Jacobi coordinates,  $\vec{\rho}$  and  $\vec{\lambda}$ , which in the case of three identical objects are

$$\begin{aligned} \vec{\rho} &= \frac{1}{\sqrt{2}}(\vec{r}_1 - \vec{r}_2) , \\ \vec{\lambda} &= \frac{1}{\sqrt{6}}(\vec{r}_1 + \vec{r}_2 - 2\vec{r}_3) . \end{aligned} \quad (19)$$

Here  $\vec{r}_1, \vec{r}_2$  and  $\vec{r}_3$  are the coordinates of the three constituents. Instead of a formulation in terms of coordinates and momenta we use the method of bosonic quantization, in which we introduce a dipole boson with  $L^P = 1^-$  for each independent relative coordinate, and an auxiliary scalar boson with  $L^P = 0^+$  [7]

$$p_{\rho,m}^\dagger, p_{\lambda,m}^\dagger, s^\dagger \quad (m = -1, 0, 1) . \quad (20)$$

The scalar boson does not represent an independent degree of freedom, but is added under the restriction that the total number of bosons  $N = n_\rho + n_\lambda + n_s$  is conserved. This procedure leads to a compact spectrum generating algebra for the radial (or orbital) excitations

$$\mathcal{G}_r = U(7) . \quad (21)$$

For a system of interacting bosons the model space is spanned by the symmetric irreducible representation  $[N]$  of  $U(7)$ . The value of  $N$  determines the size of the model space.

The mass operator depends both on the spatial and the internal degrees of freedom. We first discuss the contribution from the spatial part, which is obtained by expanding the mass-squared operator  $M^2$  in terms of the generators of  $U(7)$  [7] similar to Eq. (3), but now the boson operators  $b_{lm}^\dagger$  and  $b_{lm}$  can be any one of building blocks of Eq. (20). Because of parity conservation only interaction terms with an even number of dipole boson operators are permitted. For nonstrange  $qqq$  baryons, the mass-squared operator  $M^2$  has to be invariant under the permutation group  $S_3$ , *i.e.* under the interchange of any of the three constituent parts. This poses an additional constraint on the allowed interaction terms. The wave functions have, by construction, good angular momentum  $L$ , parity  $P$ , and permutation symmetry  $t$ . The three symmetry classes of the  $S_3$  permutation group are characterized by the irreducible representations:  $t = S$  for the one-dimensional symmetric representation,  $t = A$  for the one-dimensional antisymmetric representation, and  $t = M$  for the two-dimensional mixed symmetry representation.

### 3.2 Dynamical symmetries

The  $S_3$  invariant  $U(7)$  mass operator has a rich group structure. Just as in the case of the interacting boson model for nuclei, it is of general interest to study limiting situations, in which the mass spectrum can be obtained in closed form. These special solutions correspond to dynamical symmetries of the model. Under the restriction that the eigenstates have good angular momentum, parity and permutation symmetry, there are several possibilities. Here we consider the chains

$$U(7) \supset \left\{ \begin{array}{l} U(6) \supset \left\{ \begin{array}{l} \mathcal{SU}(3) \otimes SU(2) \supset \mathcal{SO}(3) \otimes SO(2) , \\ SO(6) \supset SU(3) \otimes SO(2) \supset \mathcal{SO}(3) \otimes SO(2) , \end{array} \right. \\ SO(7) \supset SO(6) \supset SU(3) \otimes SO(2) \supset \mathcal{SO}(3) \otimes SO(2) . \end{array} \right. \quad (22)$$

The corresponding dynamical symmetries are referred to as the  $U(6) \supset \mathcal{SU}(3) \otimes SU(2)$  limit, the  $U(6) \supset SO(6)$  limit and the  $SO(7)$  limit, respectively. These chains have the direct product group  $\mathcal{SO}(3) \otimes SO(2)$  in common, where  $\mathcal{SO}(3)$  is the angular momentum group and  $SO(2)$  is related to the permutation symmetry [7, 8, 9].

(i) The first chain corresponds to the problem of three particles in a common harmonic oscillator potential [9]. It separates the behavior in three-dimensional coordinate space determined by  $\mathcal{SU}(3) \supset \mathcal{SO}(3)$ , from that in the index space, given by  $SU(2) \supset SO(2)$ . In this limit the eigenvalues are given by

$$\begin{aligned} M^2(n, L, F, M_F) = & M_0^2 + \epsilon_1 n + \epsilon_2 n(n+5) \\ & + \alpha F(F+2) + \kappa L(L+1) + \kappa' M_F^2 . \end{aligned} \quad (23)$$

Fig. 7 shows the structure of a spectrum with  $U(6)$  symmetry. The levels are grouped into oscillator shells characterized by  $n$ . The ground state has  $n = 0$  and  $L_t^P = 0_S^+$ . The one-phonon multiplet  $n = 1$

has two degenerate states with  $L^P = 1^-$  which belong to the two-dimensional representation  $M$  of the permutation group, and the two-phonon multiplet  $n = 2$  consists of the states  $L_t^P = 2_S^+, 2_M^+, 1_A^+, 0_S^+$  and  $0_M^+$ . The splitting within an oscillator shell is determined by the last three terms of Eq. (23).

(ii) Another classification scheme for the six-dimensional oscillator is provided by the second group chain of Eq. (22). The reduction  $U(6) \supset SO(6) \supset SU(3) \otimes SO(2)$  has been studied in detail in [10]. Here it is embedded in  $U(7)$ . The spectrum of the  $U(6) \supset SO(6)$  limit is given by

$$\begin{aligned} M^2(n, \sigma, L, M_F) = & M_0^2 + \epsilon_1 n + \epsilon_2 n(n+5) \\ & + \beta \sigma(\sigma+4) + \kappa L(L+1) + \kappa' M_F^2 . \end{aligned} \quad (24)$$

Also in this case the levels are grouped into oscillator shells according to Fig. 7. However, in this case the splitting within an oscillator shell which is determined by the last three terms of Eq. (24) is different from that in the  $U(6) \supset SU(3) \otimes SU(2)$  limit.

(iii) The two group chains associated with the  $U(7) \supset U(6)$  reduction correspond a six-dimensional anharmonic oscillator, for which the total number of oscillator quanta  $n$  is a good quantum number. However, this is no longer the case for the third dynamical symmetry of Eq. (22). In the  $SO(7)$  limit the eigenvalues are

$$\begin{aligned} M^2(\omega, \sigma, L, M_F) = & M_0^2 + A(N-\omega)(N+\omega+5) \\ & + \beta \sigma(\sigma+4) + \kappa L(L+1) + \kappa' M_F^2 . \end{aligned} \quad (25)$$

Analogous to the  $SO(6)$  limit of the IBM, the  $SO(7)$  limit corresponds to a deformed oscillator. In Fig. 8 we show a typical spectrum with  $SO(7)$  symmetry. The states are now ordered in bands characterized by  $\omega$ , rather than in harmonic oscillator shells, as in the previous two examples.

### 3.3 Classical limit

A more intuitive geometric interpretation of algebraic  $U(7)$  interactions can be obtained by studying its classical limit. The procedure is similar to that discussed in Section 2.3 for the interacting boson model of nuclei. The coherent state is a condensate of  $N$  deformed bosons, which for static rotationally invariant problems can be parametrized as

$$b_c^\dagger(r, \chi, \theta) = \frac{1}{\sqrt{1+r^2}} \left[ s^\dagger + r \cos \chi p_{\lambda,x}^\dagger + r \sin \chi (\cos \theta p_{\rho,x}^\dagger + \sin \theta p_{\rho,y}^\dagger) \right] . \quad (26)$$

The geometry is chosen such that  $\vec{\rho}$  and  $\vec{\lambda}$  span the  $xy$  plane with the  $x$ -axis along  $\vec{\lambda}$  and the  $z$ -axis perpendicular to this plane. The two vectors  $\vec{\rho}$  and  $\vec{\lambda}$  are parametrized in terms of the three Euler angles which are associated with the orientation of the system, and three internal coordinates which are taken as the two lengths of the vectors  $r_\lambda = r \cos \chi$  and  $r_\rho = r \sin \chi$ , and their relative angle  $\theta$ . The hyperradius

$r$  is a measure of the dimension of the system, whereas the hyperangle  $\chi$  and the angle  $\theta$  determine its shape [11]. The surface associated with one- and two-body  $S_3$  invariant interactions is given by

$$M^2(r, \chi, \theta) = a_0 + \frac{N(N-1)}{(1+r^2)^2} [a_2 r^2 + a_4 r^4 - b r^4 \sin^2(2\chi) \sin^2 \theta] . \quad (27)$$

The coefficients  $a_i$  and  $b$  depend on the number of bosons  $N$  and the parameters in the mass-squared operator.

The classical limits of the three dynamical symmetries have a simple geometric interpretation. For the  $U(6) \supset \mathcal{SU}(3) \otimes SU(2)$  limit the surface is given by

$$\begin{aligned} M^2(r, \chi, \theta) = & M_0^2 + \epsilon_1 \frac{Nr^2}{1+r^2} + \epsilon_2 \frac{N(N-1)r^4}{(1+r^2)^2} \\ & + \alpha \frac{N(N-1)r^4}{(1+r^2)^2} [1 - \sin^2(2\chi) \sin^2 \theta] , \end{aligned} \quad (28)$$

whereas for the  $U(6) \supset SO(6)$  limit we find

$$M^2(r, \chi, \theta) = M_0^2 + \epsilon_1 \frac{Nr^2}{1+r^2} + \epsilon_2 \frac{N(N-1)r^4}{(1+r^2)^2} , \quad (29)$$

and for the  $SO(7)$  limit

$$M^2(r, \chi, \theta) = M_0^2 + A \frac{N(N-1)}{(1+r^2)^2} (1-r^2)^2 . \quad (30)$$

The surfaces for the  $U(6) \supset SO(6)$  and  $SO(7)$  limits do not depend on the angles  $\chi$  and  $\theta$ . For physical values of the parameters ( $\epsilon_1 > 0$  and  $A > 0$ ) they have a minimum at  $r = 0$  (spherical shape) and  $r^2 = 1$  (deformed shape with  $\chi$  and  $\theta$  instability), respectively. For the  $U(6) \supset \mathcal{SU}(3) \otimes SU(2)$  limit the surface depends on all three geometric variables, the radius  $r$  and the angles  $\chi$  and  $\theta$ . For realistic values of the parameters ( $\epsilon_1 > 0$ ) the minimum is at  $r = 0$  (spherical shape), just as for the  $U(6) \supset SO(6)$  limit. This analysis shows that the two  $U(6)$  limits correspond to an anharmonic vibrator, and the  $SO(7)$  limit to a deformed oscillator (or  $\chi, \theta$  unstable rotor).

It is interesting to note that the surface of Eq. (27) has another equilibrium shape, that does not correspond to one of the dynamical symmetries discussed above. We consider the operator [7, 8]

$$\begin{aligned} M^2 = & \xi_1 (R^2 s^\dagger s^\dagger - p_\rho^\dagger \cdot p_\rho^\dagger - p_\lambda^\dagger \cdot p_\lambda^\dagger) (R^2 \tilde{s} \tilde{s} - \tilde{p}_\rho \cdot \tilde{p}_\rho - \tilde{p}_\lambda \cdot \tilde{p}_\lambda) \\ & + \xi_2 \left[ (p_\rho^\dagger \cdot p_\rho^\dagger - p_\lambda^\dagger \cdot p_\lambda^\dagger) (\tilde{p}_\rho \cdot \tilde{p}_\rho - \tilde{p}_\lambda \cdot \tilde{p}_\lambda) + 4 (p_\rho^\dagger \cdot p_\lambda^\dagger) (\tilde{p}_\lambda \cdot \tilde{p}_\rho) \right] . \end{aligned} \quad (31)$$

For  $R^2 = 0$ , the mass-squared operator of Eq. (31) has  $U(7) \supset U(6)$  symmetry and corresponds to an anharmonic vibrator, whereas for  $R^2 = 1$  and  $\xi_2 = 0$  it has  $U(7) \supset SO(7)$  symmetry and corresponds to a deformed oscillator. The general case with  $R^2 \neq 0$  and  $\xi_1, \xi_2 > 0$  corresponds to an oblate symmetric top [7, 8]. This can be seen by studying the classical limit and performing a normal mode analysis. The corresponding surface

$$M^2(r, \chi, \theta) = \xi_1 \frac{N(N-1)}{(1+r^2)^2} (R^2 - r^2)^2 + \xi_2 \frac{N(N-1)r^4}{(1+r^2)^2} [1 - \sin^2(2\chi) \sin^2 \theta] , \quad (32)$$

has a stable nonlinear equilibrium shape characterized by  $r = R$ ,  $\chi = \pi/4$  and  $\theta = \pi/2$ , *i.e.* the two coordinates have equal length and are perpendicular. These two conditions are precisely those satisfied by the Jacobi coordinates of Eq. (19) for an equilateral triangle. In a normal mode analysis, the mass-squared operator of Eq. (31) reduces to leading order in  $N$  to a harmonic form, and its spectrum is given by [7, 8]

$$M^2(v_1, v_2) = \kappa_1 v_1 + \kappa_2 v_2 , \quad (33)$$

with

$$\begin{aligned} \kappa_1 &= \xi_1 4NR^2 , \\ \kappa_2 &= \xi_2 4NR^2/(1 + R^2) . \end{aligned} \quad (34)$$

Here  $v_1$  represents the number of quanta in a symmetric stretching vibration, and  $v_2 = v_{2a} + v_{2b}$  denotes the total number of quanta in a degenerate doublet which consists of an antisymmetric stretching vibration ( $v_{2a}$ ) and a bending vibration ( $v_{2b}$ ). This pattern is in agreement with the point-group classification of the fundamental vibrations of a symmetric  $X_3$  configuration [12] (see Fig. 9). Therefore, the condensate boson of Eq. (26) with  $r = R$ ,  $\chi = \pi/4$  and  $\theta = \pi/2$ , corresponds to the geometry of an oblate symmetric top with the threefold symmetry axis along the  $z$ -axis.

In Fig. 10 we show a schematic spectrum of an oblate symmetric top. In anticipation of the application to the mass spectrum of nonstrange baryon resonances we have added a term linear in the angular momentum  $L$ . The spectrum consists of a series of vibrational excitations characterized by the labels  $(v_1, v_2)$ , and a tower of rotational excitations built on top of each vibration.

The results of the analysis of the classical limit of  $S_3$  invariant one- and two-body interactions in  $U(7)$  are summarized in the phase triangle of Fig. 11, in which the three equilibrium shapes are located at the corners. This phase triangle is very similar as the one for the nuclear case: there is a spherical shape, a deformed shape that does not depend on the angular variables, and one rigid deformed shape. An important difference is that, whereas in the nuclear case there exists a large amount of collective nuclei which either correspond to one of the dynamical symmetries or to a transitional region between them, in the nucleon case there is only one single baryon spectrum. The question is now: if we assume that the radial excitations of the nucleon can be described by  $U(7)$ , where does the nonstrange baryon mass spectrum fit in this triangle?

### 3.4 Nonstrange baryons

Here we study the mass spectrum of the nonstrange baryon resonances of the nucleon (isospin  $I = 1/2$ ) and the delta (isospin  $I = 3/2$ ) family. The radial excitations are described in terms of the  $U(7)$  interacting

boson model which was discussed in the previous sections. The full algebraic structure is obtained by combining the radial part of Eq. (21) with the internal spin-flavor-color part of Eq. (16)

$$\mathcal{G} = \mathcal{G}_r \otimes \mathcal{G}_i = U(7) \otimes SU_{sf}(6) \otimes SU_c(3) . \quad (35)$$

The spatial part of the baryon wave function has to be combined with the spin-flavor and color part, in such a way that the total wave function is antisymmetric. Since the color part of the wave function is antisymmetric (color singlet), the remaining part (spatial plus spin-flavor) has to be symmetric. For nonstrange resonances which have three identical constituent parts this means that the symmetry of the spatial wave function under  $S_3$  is the same as that of the spin-flavor part. Therefore, one can use the representations of either  $S_3$  or  $SU_{sf}(6)$  to label the states. The subsequent decomposition of representations of  $SU_{sf}(6)$  into those of  $SU_f(3) \otimes SU_s(2)$  is the standard one

$$\begin{aligned} S &\leftrightarrow [56] \supset {}^28 \oplus {}^410 , \\ M &\leftrightarrow [70] \supset {}^28 \oplus {}^48 \oplus {}^210 \oplus {}^21 , \\ A &\leftrightarrow [20] \supset {}^28 \oplus {}^41 . \end{aligned} \quad (36)$$

Here the representations of the spin-flavor groups  $SU_{sf}(6)$ ,  $SU_f(3)$  and  $SU_s(2)$  are denoted by their dimensions. The total baryon wave function is expressed as

$$|\Psi\rangle = |{}^{2S+1}\dim\{SU_f(3)\}_J [\dim\{SU_{sf}(6)\}, L^P]\rangle , \quad (37)$$

where  $S$  and  $J$  are the spin and total angular momentum  $\vec{J} = \vec{L} + \vec{S}$ . The ground state baryons of Table 2 have  $L_t^P = 0_S^+$ , and are labeled by  $|{}^28_{1/2}[56, 0^+]\rangle$  for the  $J^P = 1/2^+$  octet and  $|{}^410_{3/2}[56, 0^+]\rangle$  for the  $J^P = 3/2^+$  decuplet.

We analyze the mass spectrum of nonstrange baryon resonances in terms of the mass formula

$$M^2 = M_0^2 + M_{radial}^2 + M_{sf}^2 . \quad (38)$$

The radial excitations of the nucleon are interpreted as vibrations and rotations of an oblate symmetric top [7]

$$M_{radial}^2 = \kappa_1 v_1 + \kappa_2 v_2 + \alpha L . \quad (39)$$

The N(1440) and N(1710) resonances are associated with vibrational excitations with  $(v_1, v_2) = (1, 0)$  and  $(0, 1)$ , respectively. The spin-flavor contribution to the mass-squared operator is expressed in a Gürsey-Radicati form [13]

$$M_{sf}^2 = a [\langle C_{2SU_{sf}(6)} \rangle - 45] + b [\langle C_{2SU_f(3)} \rangle - 9] + c \left[ \langle C_{2SU_s(2)} \rangle - \frac{3}{4} \right] . \quad (40)$$

According to Eq. (36), the  $SU_{sf}(6)$  term depends on the permutation symmetry of the wave functions. The  $SU_f(3)$  term only depends on the flavor, and the  $SU_s(2)$  term contains the spin dependence. A simultaneous fit to 25 well-established (3 and 4 star) nucleon and delta resonances gives a r.m.s. deviation of 39 MeV [7]. In Table 3 we show all calculated resonances below 2 GeV. Especially in the nucleon sector there are many more states calculated than have been observed so far. The lowest socalled ‘missing’ resonances correspond to the unnatural parity states with  $L^P = 1^+, 2^-$ , which are decoupled both in electromagnetic and strong decays, and hence very difficult to observe. The resonances in square brackets are not very well established experimentally (1 and 2 star) and are tentatively assigned as candidates for some of the missing states.

## 4 Summary and conclusions

In this contribution we have discussed interacting boson models of nuclear and nucleon structure. Although the energy scales involved in the two applications differ by three orders of magnitude (several MeV’s for nuclear excitations and several GeV’s for excitations of the nucleon), in both cases such algebraic models provide an elegant and, at the same time, powerful method to describe collective excitations of complex systems by introducing a set of effective degrees of freedom.

There are two advantages to these type of models that are worth mentioning. First of all, the use of algebraic techniques makes it straightforward to obtain eigenvalues and eigenvectors. This is done by means of matrix diagonalization, rather than by solving a set of coupled differential equations. Secondly, the existence of dynamical symmetries makes it possible to derive closed analytic expressions for energies, electromagnetic transition rates, decay widths and selection rules that can be tested easily by experiment, and as such they play an important role in the qualitative interpretation of the data.

A geometric interpretation of algebraic interactions has been obtained by studying its classical limit. This way it was shown that interacting boson models unify various exactly solvable models in a single framework. In the nuclear case, we showed that the three dynamical symmetries correpond to the anharmonic vibrator, the axially deformed rotor and the  $\gamma$  unstable rotor, respectively. For nonstrange baryon resonances, the  $U(7)$  model contains the (an)harmonic oscillator, the deformed oscillator and the oblate symmetric top as special limiting cases.

In conclusion, interacting boson models provide a general framework to study collective excitations of complex systems in a transparent and systematic way.

## Acknowledgements

This work is supported in part by DGAPA-UNAM under project IN101997, and by grant No. 94-00059 from the United States-Israel Binational Science Foundation.

## References

- [1] I. Talmi, ‘Simple Models of Complex Nuclei: the Shell Model and Interacting Boson Model’, Harwood Academic Publishers, 1993.
- [2] A. Bohr and B.R. Mottelson, ‘Nuclear Structure Vol. II: Nuclear Deformations’, Benjamin, 1975.
- [3] F. Iachello and A. Arima, ‘The Interacting Boson Model’, Cambridge University Press, 1987.
- [4] M. Gell-Mann and Y. Ne’eman, ‘The Eightfold Way’, Benjamin, 1964.
- [5] J.N. Ginocchio and M.W. Kirson, Phys. Rev. Lett. **44**, 1744 (1980); A.E.L. Dieperink, O. Scholten and F. Iachello, Phys. Rev. Lett. **44**, 1747 (1980); P. van Isacker and Jin-Quan Chen, Phys. Rev. C **24**, 684 (1981).
- [6] F. Iachello and R.D. Levine, ‘Algebraic theory of molecules’, Oxford University Press, 1995.
- [7] R. Bijker, F. Iachello and A. Leviatan, Ann. Phys. (N.Y.) **236**, 69 (1994).
- [8] R. Bijker, A.E.L. Dieperink, A. Leviatan, Phys. Rev. A **52**, 2786 (1995).
- [9] P. Kramer and M. Moshinsky, Nucl. Phys. **82**, 241 (1966).
- [10] E. Chacón, O. Castaños and A. Frank, J. Math. Phys. **25**, 1442 (1984).
- [11] J.L. Ballot and M. Fabre de la Ripelle, Ann. Phys. (N.Y.) **127**, 62 (1980).
- [12] G. Herzberg, ‘The spectra and structures of simple free radicals’, Dover, 1971.
- [13] F. Gürsey and L.A. Radicati, Phys. Rev. Lett. **13**, 173 (1964).
- [14] Particle Data Group, Phys. Rev. D **54**, 1 (1996).

Table 1: Model space for  $^{154}_{62}\text{Sm}_{92}$ .

---

$L^P$	Shell model [1]	IBM-1	IBM-2
$0^+$	41,654,193,517,797	16	204
$2^+$	346,132,052,934,889	26	680
$4^+$	530,897,397,260,575	30	934

---

Table 2: Classification of ground state baryons according to  $SU_f(3) \supset SU_I(2) \otimes U_Y(1)$ .

			$I$	$Y$	$Q$
$J^P = \frac{1}{2}^+$ octet	Nucleon	$N$	$\frac{1}{2}$	1	0,1
	Sigma	$\Sigma$	1	0	-1,0,1
	Lambda	$\Lambda$	0	0	0
	Xi	$\Xi$	$\frac{1}{2}$	-1	-1,0
<hr/>					
$J^P = \frac{3}{2}^+$ decuplet	Delta	$\Delta$	$\frac{3}{2}$	1	-1,0,1,2
	Sigma	$\Sigma^*$	1	0	-1,0,1
	Xi	$\Xi^*$	$\frac{1}{2}$	-1	-1,0
	Omega	$\Omega$	0	-2	-1

Table 3: All calculated nucleon and delta resonances (in MeV) below 2 GeV. Tentative assignments of 1 and 2 star resonances [14] are shown in brackets.

State	$(v_1, v_2)$	$M_{\text{calc}}$	Baryon
$^28_J[56, 0^+]$	(0,0)	939	$\text{N}(939)P_{11}$
$^28_J[70, 1^-]$	(0,0)	1566	$\text{N}(1535)S_{11}$ , $\text{N}(1520)D_{13}$
$^48_J[70, 1^-]$	(0,0)	1680	$\text{N}(1650)S_{11}$ , $\text{N}(1700)D_{13}$ , $\text{N}(1675)D_{15}$
$^28_J[20, 1^+]$	(0,0)	1720	
$^28_J[56, 2^+]$	(0,0)	1735	$\text{N}(1720)P_{13}$ , $\text{N}(1680)F_{15}$
$^28_J[70, 2^-]$	(0,0)	1875	
$^28_J[70, 2^+]$	(0,0)	1875	$[\text{N}(1900)P_{13}]$ , $[\text{N}(2000)F_{15}]$
$^48_J[70, 2^-]$	(0,0)	1972	
$^48_J[70, 2^+]$	(0,0)	1972	$[\text{N}(1990)F_{17}]$
$^28_J[56, 0^+]$	(1,0)	1440	$\text{N}(1440)P_{11}$
$^28_J[70, 1^-]$	(1,0)	1909	
$^28_J[70, 0^+]$	(0,1)	1710	$\text{N}(1710)P_{11}$
$^48_J[70, 0^+]$	(0,1)	1815	
$^28_J[56, 1^-]$	(0,1)	1866	
$^28_J[70, 1^+]$	(0,1)	1997	
$^28_J[70, 1^-]$	(0,1)	1997	
<hr/>			
$^410_J[56, 0^+]$	(0,0)	1232	$\Delta(1232)P_{33}$
$^210_J[70, 1^-]$	(0,0)	1649	$\Delta(1620)S_{31}$ , $\Delta(1700)D_{33}$
$^410_J[56, 2^+]$	(0,0)	1909	$\Delta(1910)P_{31}$ , $\Delta(1920)P_{33}$ , $\Delta(1905)F_{35}$ , $\Delta(1950)F_{37}$
$^210_J[70, 2^-]$	(0,0)	1945	$[\Delta(1940)D_{33}]$ , $\Delta(1930)D_{35}$
$^210_J[70, 2^+]$	(0,0)	1945	$[\Delta(2000)F_{35}]$
$^410_J[56, 0^+]$	(1,0)	1646	$\Delta(1600)P_{33}$
$^210_J[70, 1^-]$	(1,0)	1977	$\Delta(1900)S_{31}$
$^210_J[70, 0^+]$	(0,1)	1786	$[\Delta(1750)P_{31}]$

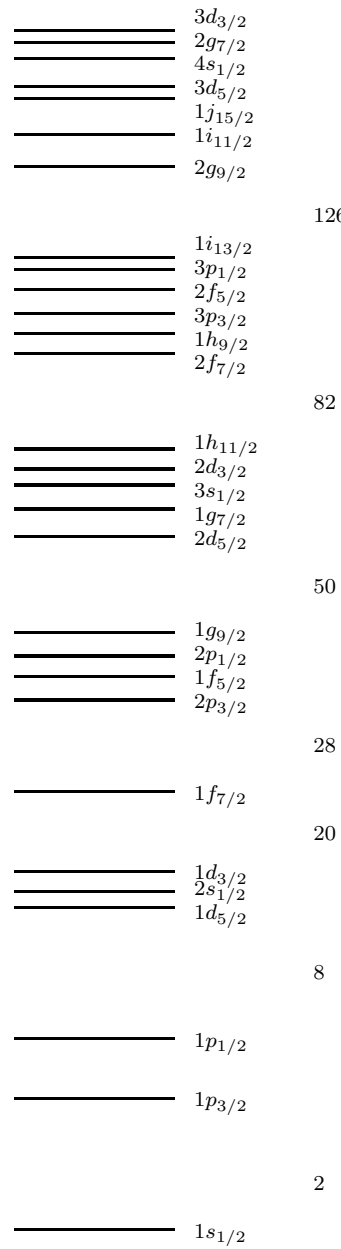


Figure 1: Single nucleon shell-model orbits and magic numbers in nuclei

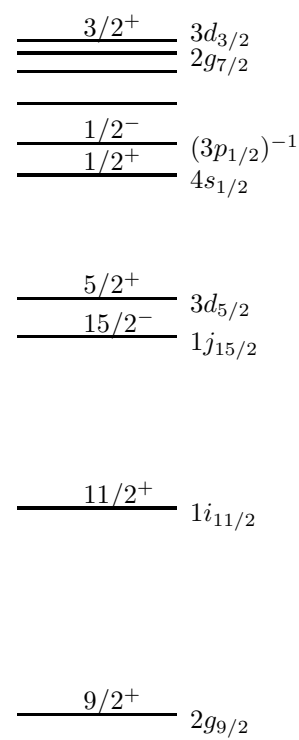


Figure 2: Single nucleon levels of  $^{209}_{82}\text{Pb}_{127}$ .

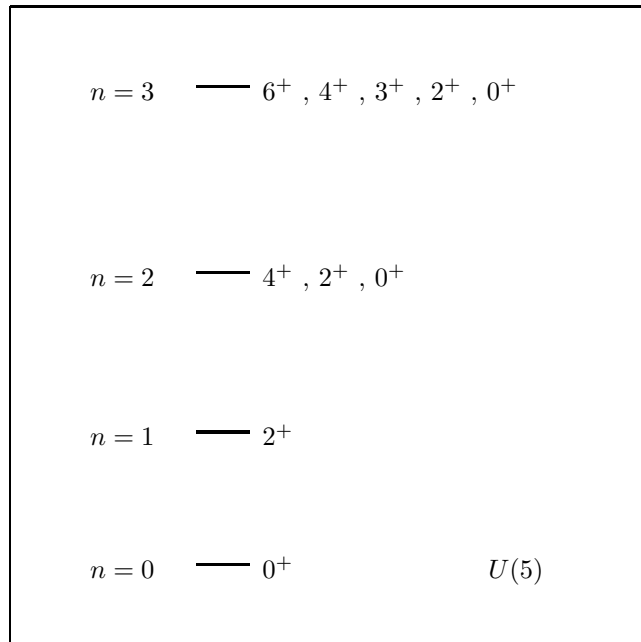


Figure 3: Schematic spectrum with  $U(5)$  symmetry. The energy levels are calculated using Eq. (5) with  $\epsilon > 0$ ,  $\alpha > 0$  and  $\beta = \gamma = 0$ . The number of bosons is  $N = 3$ .

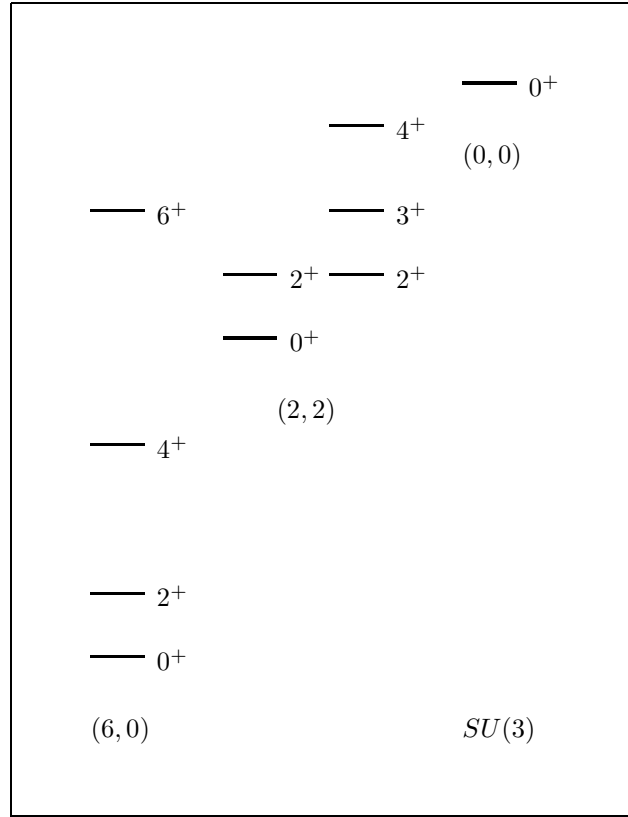
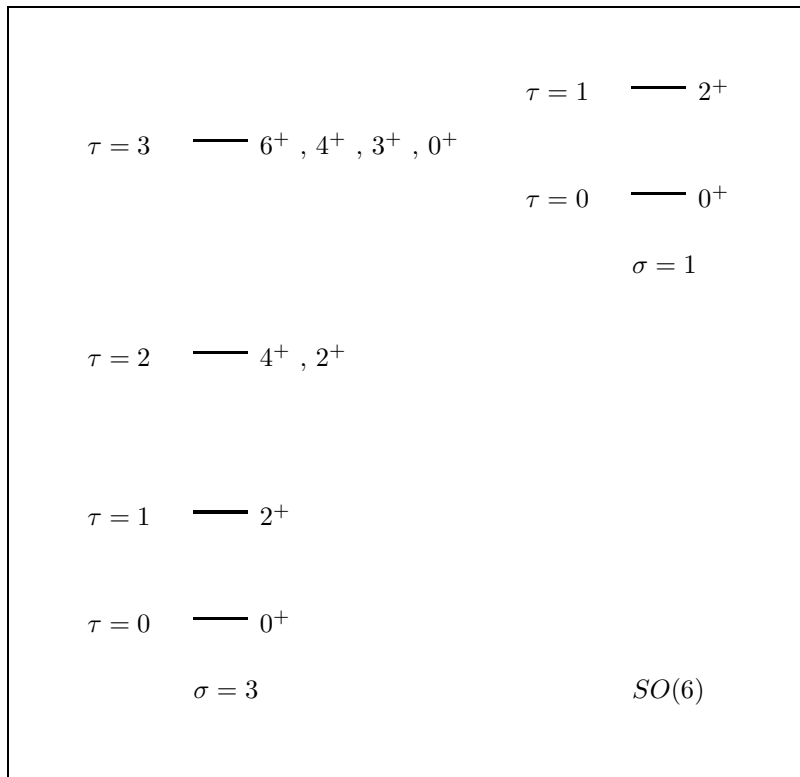
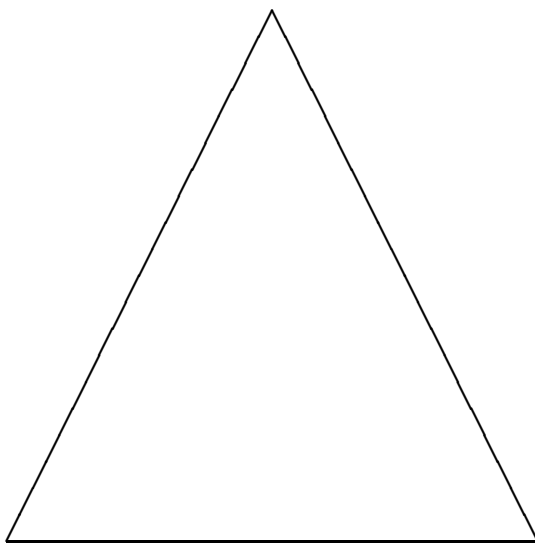


Figure 4: Schematic spectrum with  $SU(3)$  symmetry. The energy levels are calculated using Eq. (6) with  $\kappa > 0$  and  $\kappa' > 0$ . The number of bosons is  $N = 3$ . The numbers in parenthesis denote the values of  $(\lambda, \mu)$ .



Axial rotor ( $\beta > 0$ ,  $\gamma = 0$  or  $\pi/3$ )



Anharmonic  
vibrator ( $\beta = 0$ )

$\gamma$  unstable  
rotor ( $\beta > 0$ )

Figure 6: Phase triangle of the IBM.

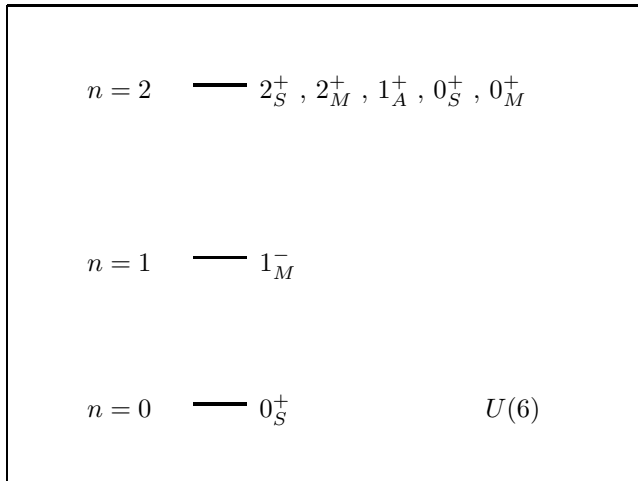


Figure 7: Schematic spectrum with  $U(6)$  symmetry. The masses are calculated using Eq. (23) with  $\epsilon_1 > 0$ ,  $\epsilon_2 > 0$  and  $\alpha = \kappa = \kappa' = 0$ . The number of bosons is  $N = 2$ .

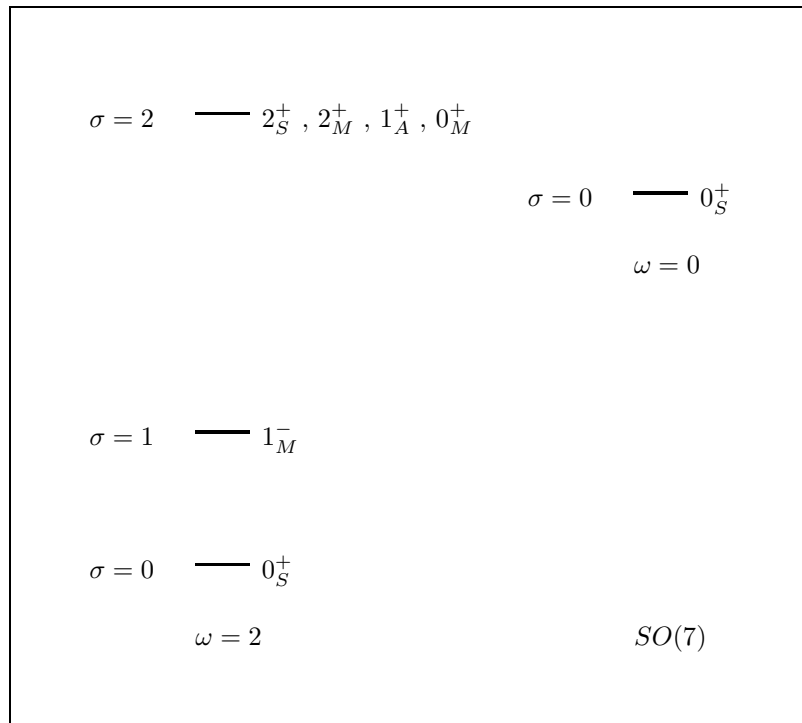


Figure 8: Schematic spectrum with  $SO(7)$  symmetry. The masses are calculated using Eq. (25) with  $A > 0$ ,  $\beta > 0$  and  $\kappa = \kappa' = 0$ . The number of bosons is  $N = 2$ .

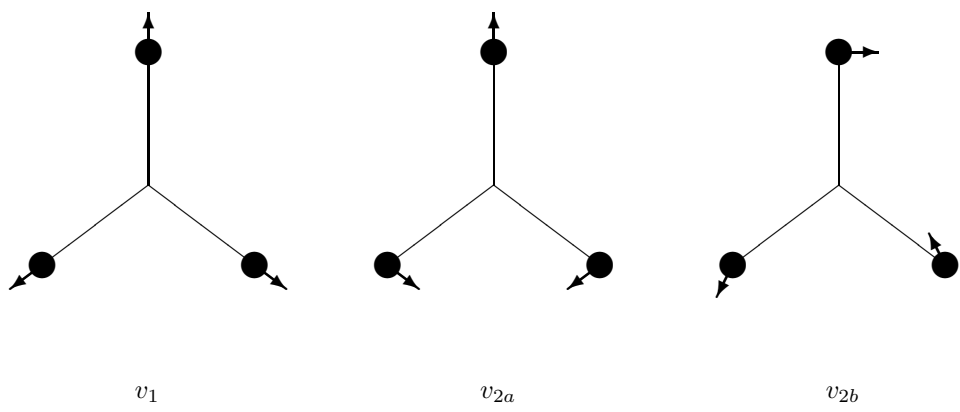


Figure 9: Fundamental vibrations of  $X_3$  configuration.

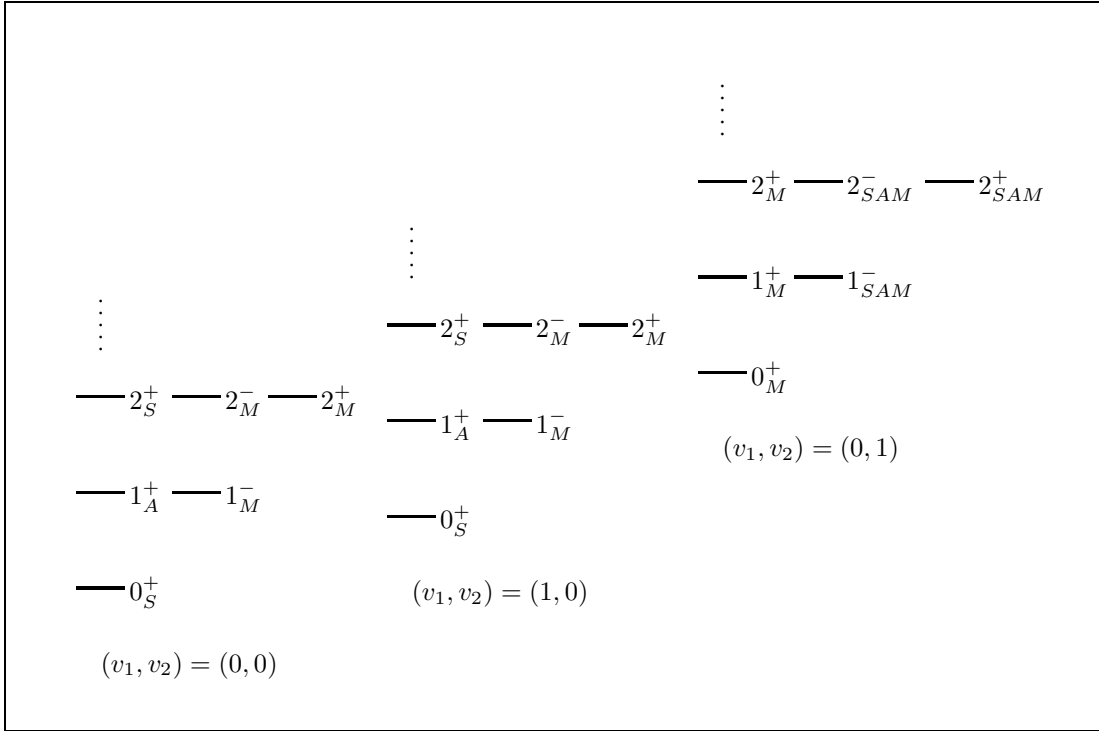
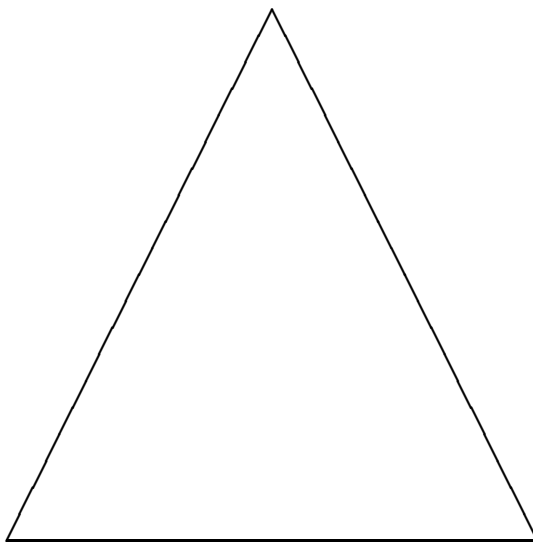


Figure 10: Schematic spectrum of an oblate symmetric top. The masses are calculated using Eq.(39) with  $\kappa_1 > 0$ ,  $\kappa_2 > 0$  and  $\alpha > 0$ .

Oblate top ( $r > 0, \chi = \pi/4, \theta = \pi/2$ )



Anharmonic  
vibrator ( $r = 0$ )

Deformed oscillator ( $r > 0$ )  
(or  $\chi, \theta$  unstable rotor)

Figure 11: Phase triangle of  $U(7)$  with  $S_3$  invariance.